(−30.0, −60.0, 15.0), $t$=4.47} demonstrated a significant negative correlation with age (Fig. 3). Even if the analysis was done on voxels with FA values higher than 0.35, to examine more anisotropic WM areas, the results were essentially unchanged (data not shown).

*3.1.3. Correlational analysis between FA values and clinical factors in schizophrenics*

There was a significant negative correlation between FA values and duration of illness in widespread WM areas (Fig. 4), while there was no significant correlation of FA values with age of onset, duration of hospitalization or daily dose of antipsychotic drugs (data not shown).

*3.2. ROI analyses*

*3.2.1. ROI-based correlational analysis in both schizophrenics and controls*

First, we constituted a General Linear Model putting diagnosis as a fixed factor and age, IQ and relative WM volume as covariates. $F$ values (significance probabilities) were as follows; diagnosis: 10.8 ($P$=0.001), age: 26.1 ($P$<0.001), IQ: 0.029 ($P$=0.865) and relative WM volume: 16.6 ($P$<0.001). Then, we added diagnosis-by-age interaction into the model. $F$ values (significance probabilities) changed as follows; diagnosis: 2.34 ($P$=0.130), age: 27.8 ($P$<0.001), IQ: 0.059 ($P$=0.809), relative WM volume: 14.1($P$<0.001) and diagnosis-by-age interaction: 7.08 ($P$=0.009). Effect of IQ was not significant in both models. There was a significant diagnosis-by-age interaction effect.

*3.2.2. ROI-based correlational analysis in controls*

Pearson's correlation coefficients (significance probabilities of the test of significance of the correlation: two-tailed) of mean WM FA value with age, IQ and relative WM volume in controls were as follows; FA vs. age: −0.287 ($P$=0.065), FA vs. IQ: −0.108 ($P$=0.496) and FA vs. mean WM volume: 0.481 ($P$=0.001). Only positive correlation between mean WM FA value and relative WM volume was statistically significant.

*3.2.3. ROI-based correlational analysis in schizophrenics*

Pearson's correlation coefficients (significance probabilities of the test of significance of the correlation: two-tailed) of mean WM FA value with clinical factors in schizophrenics were as follows; FA vs. age: −0.702 ($P$< 0.001), FA vs. duration of illness: −0.603 ($P$<0.001), FA vs. age of onset: −0.305 ($P$=0.049), FA vs. total daily dose of antipsychotics: 0.110 ($P$=0.489), FA vs. duration of hospitalization: −0.172 ($P$=0.277), FA vs. IQ: −0.064 ($P$=0.686), FA vs. relative WM volume: 0.421 ($P$=0.006). Significant positive correlation was observed between mean WM FA value and relative WM volume. Fig. 5 shows a scatter plot between age and mean WM FA value in controls and schizophrenics. Fig. 6 shows a scatter plot between duration of illness and mean WM FA value in schizophrenics. Significant negative correlations were observed between mean WM FA value and age (or duration of illness).

## 4. Discussion

In this study, we obtained three main findings; 1) lower FA values in schizophrenic patients compared with controls in WM areas including frontal and temporal WM, bilateral uncinate fasciculi (external capsules) and cingulum bundles and genu and splenium of corpus callosum, 2) age-related reductions of FA value in the widespread WM were more prominent in schizophrenics than in controls, and 3) a negative correlation between FA value in the widespread WM and duration of illness in schizophrenics.

Recent studies demonstrated age-related FA decline in normal individuals occurred in the prefrontal WM, while temporal WM were relatively preserved (Pfefferbaum et al., 2005; Salat et al., 2005). However, in this study, negative age-dependent effects were observed only in the lenient statistical threshold in the FA values of restricted areas of the WM in controls. This could be explained by the fact that all our subjects were under the age of 60, relatively less old compared to the participants of normal aging studies.

We replicated the results of the most of the previous studies, decreased FA values in the WM of schizophrenics. In the earlier studies concerning FA values in WM of patients with schizophrenia, an inherent abnormality in WM was expected to be detected since the decrease of FA values in the WM of the schizophrenic brain was assumed to occur as neurodevelopmental impairments before onset of the illness. Several studies demonstrated that schizophrenics had reduced FA value in the prefrontal WM (Buchsbaum et al., 1998), prefrontal and parieto-occipital WM (Lim et al., 1999), splenium of the corpus callosum (Agartz et al., 2001) and adjacent occipital WM (forceps major) (Agartz et al., 2001), left uncinate fasciculus and bilateral arcuate fasciculus (Burns et al., 2003), bilateral cingulum bundles (Kubicki et al., 2003). Some of them indicated that the reduction of FA values in schizophrenics might occur independently of reduction of the white matter volume. Although some studies reported no significant FA changes in schizophrenics (Steel et al., 2001; Foong et al., 2002), most studies with chronic

Please cite this article as: Takeyuki Mori et al., Progressive changes of white matter integrity in schizophrenia revealed by diffusion tensor imaging, Psychiatry Research: Neuroimaging (2007), doi:10.1016/j.pscychresns.2006.09.004

schizophrenia demonstrated lower FA values in schizophrenia (Kanaan et al., 2005). A few DTI studies have examined first episode patients (Price et al., 2005; Szeszko et al., 2005). Szeszko et al. found FA decrease in the left internal capsule and left-hemisphere WM of the middle frontal gyrus and posterior superior temporal gyrus of first-episode schizophrenics and schizoaffective disorder patients, however, the decrease was less pronounced compared with results of the majority of the studies in chronic schizophrenics. On the other hand, Price et al. reported that there was no FA decrease in the corpus callosum of patients with first-episode schizophrenia. They suggested that FA reduction in schizophrenia might reflect neuropathological abnormalities, which may occur after the onset of the disease and could be progressive. Our results, 1) age related FA reduction was more prominent in schizophrenics than controls, and 2) duration of illness was related to FA reduction in schizophrenics, suggest that changes of FA value in schizophrenia are attributable, at least in part, to progressive neuropathological changes after onset of the illness.

Contrary to our results, a previous DTI study demonstrated 'positive' correlation between age and FA in schizophrenics (Jones et al., 2006). They measured FA values of WM tracts captured from tractography, and they set seedpoints of the tracts manually from one slice of FA images. Such methods might overlook general decline of FA values in the WM. Their mean FA values (average of 8 WM tracts in each subjects) were around 0.4, which was relatively higher than those of our study {our mean FA value of entire WM was 0.35 + 0.01 (mean + S.D.)}. To simulate the analysis of the previous study, we additionally performed an analysis setting masking threshold for FA values of 0.35. As a result, the significant negative correlation remained to be present even in more anisotropic WM areas.

Previous pathological studies demonstrated microscopic abnormalities of the WM in schizophrenia such as decreased expression of myelin and oligodendrocyte-related genes, the decrease in density of oligodendrocytes (Hof et al., 2002), damage of myelin sheath lamellae (Uranova et al., 2001) and maldistribution of interstitial neurons (Akbarian et al., 1996) in prefrontal WM of the brains of schizophrenic patients. Further, a previous longitudinal MR study demonstrated progressive atrophy of the white matter in schizophrenics (Ho et al., 2003). Given these previous findings and ours, it seems likely that age-dependent FA decrease, but not increase, occurs in schizophrenic brains.

As well as a negative correlation with age, FA values of schizophrenics showed negative correlation with duration of illness but not with age of onset or daily dose of antipsychotics. The facts seem to support the hypothesis that FA reduction in schizophrenia might be associated with neuropathological abnormalities which may emerge, at least in part, after the onset of the disease and could be progressive. Further, the spatial distribution of age-related FA reduction in schizophrenics was different from those of normal individuals in previous studies that demonstrated preserved temporal white matter (Pfefferbaum et al., 2005; Salat et al., 2005). Such different distributions suggest that FA changes in schizophrenics might be associated with disease progression rather than merely exaggerated aging effects. However, it is difficult for neuroimaging studies, even for longitudinal studies, to discriminate disease progression from aging effects. The correlational study between DTI findings and pathological findings should be conducted to clarify whether reduction of FA values in schizophrenics reflect pure disease progression or merely exaggerated aging effects.

Several limitations should be considered in our study. First, our study is a cross-sectional study. To confirm progressive pathological process in the WM of the patients of schizophrenia, longitudinal studies should be conducted. Second, IQ score was not matched between groups, i.e., mean IQ score was significantly lower in schizophrenics in our samples. O'Sullivan et al. (2004) reported DTI measures were correlated strongly with cognitive decline in elderly. Thus, it could be problematic whether age-related FA decrease in our study was reflected by cognitive decline. However, no significant correlation was observed between mean WM FA values and IQ in our sample. Also, regarding schizophrenia, it has been hypothesized that most cognitive change takes place early in their psychotic episodes and it remains relatively stable through long term in the illness (Hoff et al., 2005). Hence, at least from our data, we cannot attribute age-related FA decline in schizophrenia to IQ changes. Third, the issue of partial volume effect should be addressed. In schizophrenia, progressive WM atrophy has been reported in the previous studies (Ho et al., 2003). Due to the atrophy, it is possible that the voxels located in the border of the WM and other tissues in schizophrenics were estimated as having lower FA values. However, we minimized the problem by using the high dimensional warping algorithm, threshold masking for FA values and adopting relative WM volume as a nuisance variable. Another issue is the possible effect of long-term medication with antipsychotics. Although daily dose of antipsychotics was not correlated with FA values in schizophrenics, we could not estimate accurate cumulative doses of antipsychotics

Please cite this article as: Takeyuki Mori et al., Progressive changes of white matter integrity in schizophrenia revealed by diffusion tensor imaging, Psychiatry Research: Neuroimaging (2007), doi:10.1016/j.pscychresns.2006.09.004

throughout the duration of illness. Several morphological MR studies and animal studies suggested that the administration of antipsychotics could affect brain morphology (Wang et al., 2004; Lieberman et al., 2005). It is possible that long-term medication with antipsychotics also affects microstructure of the WM in schizophrenics. The longitudinal animal studies may clarify this issue.

In conclusion, we confirmed decreased FA in schizophrenics, compared to controls in the widespread WM areas in a Japanese sample. We found that age-dependent FA decline was more pronounced in chronic schizophrenics compared to controls, and that such FA decline was significantly correlated with duration of illness in patients. These observations suggest that decreased FA values in schizophrenia might be attributable, at least in part, to progressive changes in the WM after the onset of the illness.

## Acknowledgment

We appreciate Osamu Takizawa (Siemens-Asahi Medical Technologies, Tokyo, Japan) for supporting to develop a program for calculation of FA values. This work was supported in part by Grants-in-Aid from the Japanese Ministry of Health, Labor and Welfare (H17-kokoro-007 and H16-kokoro-002, the Research Grant for Nervous and Mental Disorders 17B-2), the Japanese Ministry of Education, Culture, Sports, Science and Technology, Core research for Evolutional Science and Technology of Japan Science and Technology Agency and Japan Foundation for Neuroscience and Mental Health.

## References

Agartz, I., Andersson, J.L., Skare, S., 2001. Abnormal brain white matter in schizophrenia: a diffusion tensor imaging study. NeuroReport 12, 2251–2254.

Akbarian, S., Kim, J.J., Potkin, S.G., Hetrick, W.P., Bunney Jr., W.E., Jones, E.G., 1996. Maldistribution of interstitial neurons in prefrontal white matter of the brains of schizophrenic patients. Archives of General Psychiatry 53, 425–436.

American Psychiatric Association, 1994. Diagnostic and Statistical Manual of Mental Disorders: DSM-IV. American Psychiatric Association, Washington, DC, p. xxvii, 886 pp.

Andreasen, N.C., O'Leary, D.S., Flaum, M., Nopoulos, P., Watkins, G.L., Boles Ponto, L.L., Hichwa, R.D., 1997. Hypofrontality in schizophrenia: distributed dysfunctional circuits in neuroleptic-naive patients. Lancet 349, 1730–1734.

Ashburner, J., Andersson, J.L., Friston, K.J., 1999. High-dimensional image registration using symmetric priors. NeuroImage 9, 619–628.

Basser, P.J., 1995. Inferring microstructural features and the physiological state of tissues from diffusion-weighted images. NMR in Biomedicine 8, 333–344.

Basser, P.J., Mattiello, J., LeBihan, D., 1994. MR diffusion tensor spectroscopy and imaging. Biophysical Journal 66, 259–267.

Buchsbaum, M.S., Tang, C.Y., Peled, S., Gudbjartsson, H., Lu, D., Hazlett, E.A., Downhill, J., Haznedar, M., Fallon, J.H., Atlas, S.W., 1998. MRI white matter diffusion anisotropy and PET metabolic rate in schizophrenia. NeuroReport 9, 425–430.

Bullmore, E.T., Frangou, S., Murray, R.M., 1997. The dysplastic net hypothesis: an integration of developmental and dysconnectivity theories of schizophrenia. Schizophrenia Research 28, 143–156.

Burns, J., Job, D., Bastin, M.E., Whalley, H., Macgillivray, T., Johnstone, E.C., Lawrie, S.M., 2003. Structural disconnectivity in schizophrenia: a diffusion tensor magnetic resonance imaging study. The British Journal of Psychiatry 182, 439–443.

Cannon, T.D., van Erp, T.G., Huttunen, M., Lonnqvist, J., Salonen, O., Valanne, L., Poutanen, V.P., Standertskjold-Nordenstam, C.G., Gur, R.E., Yan, M., 1998. Regional gray matter, white matter, and cerebrospinal fluid distributions in schizophrenic patients, their siblings, and controls. Archives of General Psychiatry 55, 1084–1091.

Christiansen, P., Larsson, H.B., Thomsen, C., Wieslander, S.B., Henriksen, O., 1994. Age dependent white matter lesions and brain volume changes in healthy volunteers. Acta Radiologica 35, 117–122.

Davis, K.L., Stewart, D.G., Friedman, J.I., Buchsbaum, M., Harvey, P.D., Hof, P.R., Buxbaum, J., Haroutunian, V., 2003. White matter changes in schizophrenia: evidence for myelin-related dysfunction. Archives of General Psychiatry 60, 443–456.

Foong, J., Symms, M.R., Barker, G.J., Maier, M., Miller, D.H., Ron, M.A., 2002. Investigating regional white matter in schizophrenia using diffusion tensor imaging. NeuroReport 13, 333–336.

Friston, K.J., Holmes, A.P., Poline, J.B., Grasby, P.J., Williams, S.C., Frackowiak, R.S., Turner, R., 1995. Analysis of fMRI time-series revisited. NeuroImage 2, 45–53.

Frith, C., Dolan, R., 1996. The role of the prefrontal cortex in higher cognitive functions. Brain Research. Cognitive Brain Research 5, 175–181.

Good, C.D., Johnsrude, I.S., Ashburner, J., Henson, R.N., Friston, K.J., Frackowiak, R.S., 2001. A voxel-based morphometric study of ageing in 465 normal adult human brains. NeuroImage 14, 21–36.

Ho, B.C., Andreasen, N.C., Nopoulos, P., Arndt, S., Magnotta, V., Flaum, M., 2003. Progressive structural brain abnormalities and their relationship to clinical outcome: a longitudinal magnetic resonance imaging study early in schizophrenia. Archives of General Psychiatry 60, 585–594.

Hof, P.R., Haroutunian, V., Copland, C., Davis, K.L., Buxbaum, J.D., 2002. Molecular and cellular evidence for an oligodendrocyte abnormality in schizophrenia. Neurochemical Research 27, 1193–1200.

Hoff, A.L., Svetina, C., Shields, G., Stewart, J., DeLisi, L.E., 2005. Ten year longitudinal study of neuropsychological functioning subsequent to a first episode of schizophrenia. Schizophrenia Research 78, 27–34.

Jones, D.K., Symms, M.R., Cercignani, M., Howard, R.J., 2005. The effect of filter size on VBM analyses of DT-MRI data. NeuroImage 26, 546–554.

Jones, D.K., Catani, M., Pierpaoli, C., Reeves, S.J., Shergill, S.S., O'Sullivan, M., Golesworthy, P., McGuire, P., Horsfield, M.A., Simmons, A., Williams, S.C., Howard, R.J., 2006. Age effects on diffusion tensor magnetic resonance imaging tractography measures of frontal cortex connections in schizophrenia. Human Brain Mapping 27, 230–238.

Please cite this article as: Takeyuki Mori et al., Progressive changes of white matter integrity in schizophrenia revealed by diffusion tensor imaging, Psychiatry Research: Neuroimaging (2007), doi:10.1016/j.pscychresns.2006.09.004

Kanaan, R.A., Kim, J.S., Kaufmann, W.E., Pearlson, G.D., Barker, G.J., McGuire, P.K., 2005. Diffusion tensor imaging in schizophrenia. Biological Psychiatry 58, 921–929.

Kubicki, M., Westin, C.F., Nestor, P.G., Wible, C.G., Frumin, M., Maier, S.E., Kikinis, R., Jolesz, F.A., McCarley, R.W., Shenton, M.E., 2003. Cingulate fasciculus integrity disruption in schizophrenia: a magnetic resonance diffusion tensor imaging study. Biological Psychiatry 54, 1171–1180.

Lieberman, J.A., Tollefson, G.D., Charles, C., Zipursky, R., Sharma, T., Kahn, R.S., Keefe, R.S., Green, A.I., Gur, R.E., McEvoy, J., Perkins, D., Hamer, R.M., Gu, H., Tohen, M., 2005. Antipsychotic drug effects on brain morphology in first-episode psychosis. Archives of General Psychiatry 62, 361–370.

Lim, K.O., Hedehus, M., Moseley, M., de Crespigny, A., Sullivan, E.V., Pfefferbaum, A., 1999. Compromised white matter tract integrity in schizophrenia inferred from diffusion tensor imaging. Archives of General Psychiatry 56, 367–374.

Maldjian, J.A., Laurienti, P.J., Kraft, R.A., Burdette, J.H., 2003. An automated method for neuroanatomic and cytoarchitectonic atlas-based interrogation of fMRI data sets. NeuroImage 19, 1233–1239.

Meier-Ruge, W., Ulrich, J., Bruhlmann, M., Meier, E., 1992. Age-related white matter atrophy in the human brain. Annals of the New York Academy of Sciences 673, 260–269.

Miyakawa, T., Sumiyoshi, S., Deshimaru, M., Suzuki, T., Tomonari, H., 1972. Electron microscopic study on schizophrenia. Mechanism of pathological changes. Acta Neuropathologica 20, 67–77.

Nusbaum, A.O., Tang, C.Y., Buchsbaum, M.S., Wei, T.C., Atlas, S.W., 2001. Regional and global changes in cerebral diffusion with normal aging. AJNR American Journal of Neuroradiology 22, 136–142.

O'Sullivan, M., Jones, D.K., Summers, P.E., Morris, R.G., Williams, S.C., Markus, H.S., 2001. Evidence for cortical "disconnection" as a mechanism of age-related cognitive decline. Neurology 57, 632–638.

O'Sullivan, M., Morris, R.G., Huckstep, B., Jones, D.K., Williams, S.C., Markus, H.S., 2004. Diffusion tensor MRI correlates with executive dysfunction in patients with ischaemic leukoaraiosis. Journal of Neurology, Neurosurgery and Psychiatry 75, 441–447.

Pfefferbaum, A., Sullivan, E.V., Hedehus, M., Adalsteinsson, E., Lim, K.O., Moseley, M., 2000a. In vivo detection and functional correlates of white matter microstructural disruption in chronic alcoholism. Alcoholism, Clinical and Experimental Research 24, 1214–1221.

Pfefferbaum, A., Sullivan, E.V., Hedehus, M., Lim, K.O., Adalsteinsson, E., Moseley, M., 2000b. Age-related decline in brain white matter anisotropy measured with spatially corrected echo-planar diffusion tensor imaging. Magnetic Resonance in Medicine 44, 259–268.

Pfefferbaum, A., Adalsteinsson, E., Sullivan, E.V., 2005. Frontal circuitry degradation marks healthy adult aging: Evidence from diffusion tensor imaging. NeuroImage 26, 891–899.

Price, G., Bagary, M.S., Cercignani, M., Altmann, D.R., Ron, M.A., 2005. The corpus callosum in first episode schizophrenia: a diffusion tensor imaging study. Journal of Neurology, Neurosurgery and Psychiatry 76, 585–587.

Salat, D.H., Kaye, J.A., Janowsky, J.S., 1999. Prefrontal gray and white matter volumes in healthy aging and Alzheimer disease. Archives of Neurology 56, 338–344.

Salat, D.H., Tuch, D.S., Greve, D.N., van der Kouwe, A.J., Hevelone, N.D., Zaleta, A.K., Rosen, B.R., Fischl, B., Corkin, S., Rosas, H.D., Dale, A.M., 2005. Age-related alterations in white matter microstructure measured by diffusion tensor imaging. Neurobiology of Aging 26, 1215–1227.

Steel, R.M., Bastin, M.E., McConnell, S., Marshall, I., Cunningham-Owens, D.G., Lawrie, S.M., Johnstone, E.C., Best, J.J., 2001. Diffusion tensor imaging (DTI) and proton magnetic resonance spectroscopy (1H MRS) in schizophrenic subjects and normal controls. Psychiatry Research 106, 161–170.

Szeszko, P.R., Ardekani, B.A., Ashtari, M., Kumra, S., Robinson, D.G., Sevy, S., Gunduz-Bruce, H., Malhotra, A.K., Kane, J.M., Bilder, R.M., Lim, K.O., 2005. White matter abnormalities in first-episode schizophrenia or schizoaffective disorder: a diffusion tensor imaging study. The American Journal of Psychiatry 162, 602–605.

Uranova, N., Orlovskaya, D., Vikhreva, O., Zimina, I., Kolomeets, N., Vostrikov, V., Rachmanova, V., 2001. Electron microscopy of oligodendroglia in severe mental illness. Brain Research Bulletin 55, 597–610.

Uranova, N.A., Vostrikov, V.M., Orlovskaya, D.D., Rachmanova, V.I., 2004. Oligodendroglial density in the prefrontal cortex in schizophrenia and mood disorders: a study from the Stanley Neuropathology Consortium. Schizophrenia Research 67, 269–275.

Wang, H.D., Dunnavant, F.D., Jarman, T., Deutch, A.Y., 2004. Effects of antipsychotic drugs on neurogenesis in the forebrain of the adult rat. Neuropsychopharmacology 29, 1230–1238.

Please cite this article as: Takeyuki Mori et al., Progressive changes of white matter integrity in schizophrenia revealed by diffusion tensor imaging, Psychiatry Research: Neuroimaging (2007), doi:10.1016/j.pscychresns.2006.09.004

*The World Journal of Biological Psychiatry*, 2007; 00(0): 0–00

BRIEF REPORT

# Abnormal microstructures of the basal ganglia in schizophrenia revealed by diffusion tensor imaging

RYOTA HASHIMOTO[1–3], TAKEYUKI MORI[3,4], KIYOTAKA NEMOTO[4], YOSHIYA MORIGUCHI[4], HIROKO NOGUCHI[3], TETSUO NAKABAYASHI[5], HIROAKI HORI[3], SEIICHI HARADA[5], HIROSHI KUNUGI[3], OSAMU SAITOH[5] & TAKASHI OHNISHI[3,4,6]

[1]*The Osaka-Hamamatsu Joint Research Center For Child Mental Development, Osaka University Graduate School of Medicine,* [2]*Department of Psychiatry, Osaka University Graduate School of Medicine,* [3]*Department of Mental Disorder Research, National Institute of Neuroscience, National Center of Neurology and Psychiatry,* [4]*Department of Radiology, National Center Hospital for Mental, Nervous, and Muscular Disorders, National Center of Neurology and Psychiatry,* [5]*Department of Psychiatry, National Center Hospital for Mental, Nervous, and Muscular Disorders, National Center of Neurology and Psychiatry, and* [6]*Department of Investigative Radiology, Research Institute, National Cardiovascular Center, Osaka, Japan*

**Abstract**

There has been a hypothesis that deficits in the basal ganglia–thalamic system may play an important role in the dysfunctional goal-directed behaviour in schizophrenia. By using diffusion tensor imaging, we measured fractional anisotropy (FA) values in the basal ganglia–thalamic system in 42 schizophrenics and 42 matched controls to investigate microstructural tissue alterations in the basal ganglia–thalamic system in schizophrenia. Schizophrenics had significantly lower FA values in the bilateral globus pallidus and left thalamus compared to controls, suggesting that schizophrenics might have microstructural abnormalities in globus pallidus and thalamus. These data support the notion that myelination abnormalities in basal ganglia–thalamic system are related to the pathophysiology of schizophrenia.

**Key words:** *Schizophrenia, diffusion tensor imaging, basal ganglia, globus pallidus, MRI*

## Introduction

Schizophrenia often demonstrated movement abnormalities, such as catatonia, pacing and other stereotyped behaviours considered to be associated with basal ganglia dysfunction. The basal ganglia regulates not only motor behaviours but also aspects of cognitive and limbic behaviours. There has been a hypothesis that deficits in the basal ganglia–thalamic system may play an important role in the dysfunctional goal-directed behaviour in schizophrenia (Andreasen 1999). In fact, several studies demonstrated abnormalities in the basal ganglia in schizophrenic brains, including the volume reductions of the pallidum internum of postmortem brains of patients with schizophrenia (Bogerts et al. 1985), higher volumes in the globus pallidus of previously treated patients with schizophrenia than the healthy comparison subjects and the neuroleptic-naive patients (Gur et al. 1998), fMRI evidence for basal ganglia dysfunction in subjects with schizophrenia (Menon et al. 2001), abnormality of oligodendroglial cells in caudate nucleus in schizophrenia (Uranova et al. 2001), and positive correlation between globus pallidus and the severity of global symptoms in neuroleptic-naive patients (Spinks et al. 2005).

Diffusion tensor imaging (DTI) is a relatively new technique, and it is useful for evaluating white matter abnormalities in schizophrenia. We have reported progressive changes of white matter integrity in schizophrenia using DTI (Mori et al. 2007).

Correspondence: Ryota Hashimoto, MD, The Osaka-Hamamatsu Joint Research Center for Child Mental Development, Osaka University Graduate School of Medicine, D3, 2-2, Yamadaoka, Suita, Osaka, 565-0871, Japan. Tel: +81 6 6879 3074. Fax: +81 6 6879 3059. E-mail: hashimor@psy.med.osaka-u.ac.jp

*(Received 4 July 2007; accepted 17 October 2007)*

ISSN 1562-2975 print/ISSN 1814-1412 online 
DOI: 10.1080/15622970701762536

Recently, this technique was applied to investigate abnormalities of the subcortical regions in neurodegenerative diseases. Patients with Parkinson's disease had significantly decreased fractional anisotropy (FA) in the region of interest along a line between the substantia nigra and the lower part of the putamen/caudate complex, in which the nigrostriatal dopaminergic neurons are lost in Parkinson's disease, demonstrating its possibility to detect microstructural tissue alterations (Yoshikawa et al. 2004). To investigate possible microstructural abnormalities in the basal ganglia–thalamic system in schizophrenia, we measured FA values in the basal ganglia and the thalami in schizophrenics and in normal controls for comparison, as a sub-analysis of our previous study (Mori et al. 2007).

## Material and methods

### *Subjects and clinical assessments*

Forty-two patients with DSM-IV schizophrenia (26 male and 16 female, one left hander, mean age: 40.0 ± 9.3 years old, education: 13.0 ± 2.9 years, mean duration of illness; 16.8 ± 9.0 years, mean daily dose of antipsychotics (chlorpromazine equivalent): 1005.1 ± 735.3 mg/day) (Association 1994) and 42 controls (26 male and 16 female, one left hander, mean age: 39.2 ± 9.0 years old, education: 17.1 ± 3.5 years) were participated in our study. Written informed consent was obtained from all the subjects. This study has been approved by the local ethics committee and has therefore been performed in accordance with the ethical standards laid down in the 1964 Declaration of Helsinki. All the normal subjects were screened by a questionnaire on medical history and excluded if they had neurological, psychiatric or medical conditions that could potentially affect the central nervous system. We employed the Japanese version of National Adult Reading Test (JART) as a convenient tool to measure IQ for participants (premorbid IQ for schizophrenics). Patients had fewer years of education (two-sample $t$-test, $P < 0.0001$), lower scores of JART (controls: 78.8 ± 11.5, schizophrenics: 58.7 ± 25.3, two-sample $t$-test $P < 0.001$).

### *Neuroimaging analysis*

MR studies were performed on a 1.5-Tesla Siemens Magnetom Vision Plus system. Axial DTI scans aligned to the plane containing anterior and posterior commissures were acquired with a pulsed-gradient, spin-echo, single-shot echo planar imaging (EPI) sequence (TR/TE = 4000/100 ms, 256 × 256 matrix, FOV 240 mm, $b = 1000$ s/mm$^2$, NEX = 4, 20 slices, 5 mm slice thickness, 1.5 mm gap). Diffusion was measured along six non-collinear directions, because six directions were maximum number of this Vision Plus system. For each of six gradient directions, four acquisitions were averaged. Four acquisitions without diffusion weighting ($b = 0$) were also averaged. Additionally, a three-dimensional volumetric acquisition of a T1-weighted gradient echo sequence with a gapless series of thin sagittal sections using an MPRage sequence (TR/TE = 11.4/4.4 ms; flip angle, 15°; acquisition matrix, 256 × 256; NEX = 1, FOV 315 mm; slice thickness 1.23 mm) was acquired for evaluating the volume of grey matter (GM), WM and cerebrospinal fluid (CSF) space. Seven diffusion images acquired as above by an in-house script described previously (Mori et al. 2007) on Matlab 6.5 software (Mathworks, Inc., MA, USA). Then, the FA images were spatially normalized using high-dimensional-warping algorithm (Ashburner et al. 1999) and were matched to the FA template image (Figure 1, top). To make the FA template image, we warped FA images of four normal subjects (other than 42 control subjects) to the single-subject T1 template (skull stripped image) using spatial normalization function of SPM2 and averaged the four warped FA images. The transformed FA images were smoothed with a Gaussian kernel (the filter size, full-width half-maximum: 6 × 6 × 6 mm).

Since our interest was FA changes in the basal ganglia and thalamus, we excluded other brain areas by using an explicit mask (Figure 1, top). The resultant FA maps were analyzed using Statistical parametric mapping 2 (SPM2), which implements a 'general linear model'. To test hypotheses about regional population effects, data were analyzed by a two-sample $t$-test without global normalization. JART scores were treated as nuisance variables. Furthermore, we performed correlational analyses between duration of illness, age of onset, total daily dose of antipsychotic drugs (chlorpromazine equivalent) and FA value in the schizophrenics. Our a priori hypothesis is limited to the basal ganglia; however, investigation of the FA changes within this ROI is null hypothesis. Thus, we used $P < 0.05$, corrected for multiple comparisons with Family–Wise Error rate (FWE) within basal ganglia as a statistical threshold.

## Results

In comparison with controls, schizophrenics had significantly lower FA values in the bilateral globus pallidus (GP) (Figure 1, bottom). Increased FA values in schizophrenics were not found in any regions (data not shown).

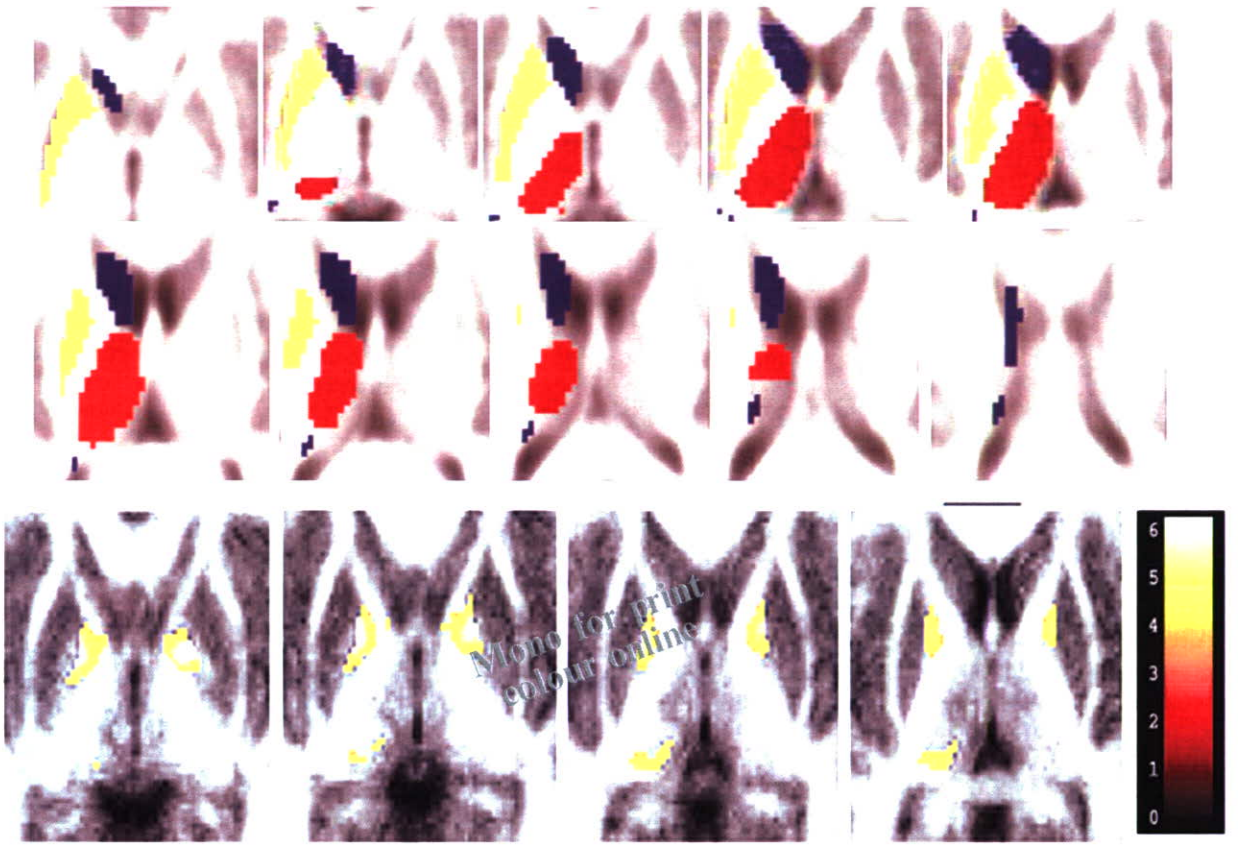


Figure 1. Top: A half of the explicit mask is displayed onto mean FA images of warped FA images obtained from 42 controls (dark blue: caudate nucleus; yellow: putamen; light blue: globus pallidus; red: thalamus). Even after averaging, the mean images are not blurred. Since globus pallidus is traversed by numerous myelinated nerve fibres, it shows higher FA value than other parts of basal ganglia. Bottom: The SPM {t} is displayed onto mean axial FA images of 42 schizophrenics. A significant reduction of FA value in schizophrenia was noted in the bilateral globus pallidus (right GP: $t$ value = 6.52, Talairach coordinate $x$, $y$, $z$: 18, −2, −2, left GP: $t$ value = 6.37, Talairach coordinate $x$, $y$, $z$: −18, −3, −2) and left thalamus ($t$ value = 4.96, Talairach coordinate $x$, $y$, $z$: −18, −33, 10).

A correlational analysis in the schizophrenics demonstrated a significantly negative correlation between duration of illness and FA in the left head of the caudate nucleus ($t$ value = 4.77, Talairach coordinate $x$, $y$, $z$: −11, −17, −6). However, there is no significant correlation between duration of illness and FA values in the GP and the thalamus. There was no significant correlation between FA values in the basal ganglia–thalamic system with age of onset or total daily dose of antipsychotic drugs.

## Discussion

In this study, we found a significantly reduced FA value in the bilateral GP and left thalamus in schizophrenics compared to controls. We consider that reduced FA may reflect microstructural abnormalities in the basal ganglia–thalamic system in schizophrenia. A previous fMRI study suggested that GP itself may be the primary locus of the functional deficits in the basal ganglia and may be dysfunctional in schizophrenia (Menon et al. 2001). A postmortem study of basal ganglia morphology reported that only the GP were smaller in schizophrenics than in controls (Bogerts et al. 1985). These studies indicated functional and structural abnormalities in GP in schizophrenia. Our data, reduced FA in GP in schizophrenia, were obtained using a size-adjusted high-dimensional warping method (Ohnishi et al. 2006). Our results, microstructural abnormalities in the GP in schizophrenia, are consistent with previous reports.

Although the underlying mechanisms remain to be clarified, previous DTI studies in parkinsonism have well demonstrated ongoing pathological changes in neurodegenerative diseases, suggesting that this technique has the potential to detect microstructural alterations in the basal ganglia (Yoshikawa et al. 2004). Since pathological findings of schizophrenia are still ambiguous, the underlying pathological changes of reduced FA values in schizophrenia are unclear. However, multiple lines

of evidence now converge to implicate oligodendroglia and myelin in schizophrenia (Davis et al. 2003). We assume that damage of myelinated nerve fibres may contribute to FA reduction in the basal ganglia–thalamic system. The GP is traversed by numerous myelinated nerve fibres that give it the pale appearance for which it is named, and has rich connections to the putamen and the thalamus. These histological characteristics of the GP may contribute to its higher FA values. A qualitative electron microscopic study reported the density of concentric lamellar bodies (an indicator of damage of myelinated fibres) was dramatically increased in the caudate nucleus in schizophrenia, as compared to controls (Uranova et al. 2001). Such pathological changes seem to explain decreased FA values in the schizophrenic brain. However, there have been no data on whether GP also have alterations of myelinated fibres. Further pathological studies need to be conducted to draw a firm conclusion on this matter.

Although some studies demonstrated abnormalities of GP in neuroleptic-naïve schizophrenics (Spinks et al. 2005), abnormalities in the basal ganglia have been considered to relate to antipsychotic medication (Gur et al. 1998). In this study, FA changes in the GP and thalamus were not associated with the duration of illness or the daily dose of antipsychotic drugs, suggesting that FA changes in these regions might be independent of medication with neuroleptics. Guidelines for the biological treatment of schizophrenia developed by an international Task Force of the World Federation of Societies of Biological Psychiatry recommended atypical antipsychotics as first line drugs (Falkai et al. 2005, 2006). The differential treatment effects on brain morphology could be due to typical antipsychotics-associated toxicity or greater therapeutic effects of atypical antipsychotics (Lieberman et al. 2005). It would be interesting to compare patients treated with atypical antipsychotics to those with a history of typical antipsychotics treatment; however; the subgroup of patients that were only treated with atypical antipsychotics or the subgroup of patients that were only treated with typical antipsychotics were too small to investigate a possible difference between two groups in FA in our sample. To conclude whether observed change of FA value is a result of medication or relates to the pathophysiology of schizophrenia itself, longitudinal studies on treated schizophrenics, and studies on neuroleptic-naive schizophrenics should be conducted.

There is a limitation to our study: we used a 1.5-Tesla Siemens Magnetom Vision Plus system, which is a relatively old system. We chose six gradient directions, which is quite low, as this number is the maximum number of directions in this system. Slice thickness of 5 mm and 1.5-mm slice gaps are methodological drawbacks to this study. The reason why we used a slice thickness of 5 mm and 1.5-mm slice gaps is to cover the whole brain as in our previous study (Mori et al. 2007). There may be a partial volume effect in our mapping parameters, although we minimized the problem by using the high-dimensional warping algorithm.

Our data suggest that patients with schizophrenia might have microstructural abnormalities in globus pallidus and thalamus. The DTI study may be a promising method to investigate microstructural abnormalities in schizophrenia.

## Acknowledgements/Statement of interest

We are grateful to Osamu Takizawa (Siemens) for supporting the development of a program for calculation of FA values. This work was supported in part by Grants-in-Aid from the Japanese Ministry of Health, Labor and Welfare (H17-kokoro-007 and H16-kokoro-002), the Japanese Ministry of Education, Culture, Sports, Science and Technology, and Core research for Evolutional Science and Technology of Japan Science and Technology Agency, Japan Foundation for Neuroscience and Mental Health.

## References

Andreasen NC. 1999. A unitary model of schizophrenia: Bleuler's 'fragmented phrene' as schizencephaly. Arch Gen Psychiatry 56:781–787.

Ashburner J, Andersson JL, Friston KJ. 1999. High-dimensional image registration using symmetric priors. Neuroimage 9:619–628.

American Psychiatric Association. 1994. Diagnostic and statistical manual of mental disorders. 4th ed. (DSM-IV). Washington, DC: American Psychiatric Association.

Bogerts B, Meertz E, Schonfeldt-Bausch R. 1985. Basal ganglia and limbic system pathology in schizophrenia. A morphometric study of brain volume and shrinkage. Arch Gen Psychiatry 42:784–791.

Davis KL, Stewart DG, Friedman JI, et al. 2003. White matter changes in schizophrenia: evidence for myelin-related dysfunction. Arch Gen Psychiatry 60:443–456.

Falkai P, Wobrock T, Lieberman J, Glenthoj B, Gattaz WF, Moller HJ. 2005. World Federation of Societies of Biological Psychiatry (WFSBP) guidelines for biological treatment of schizophrenia, Part 1: acute treatment of schizophrenia. World J Biol Psychiatry 6:132–191.

Falkai P, Wobrock T, Lieberman J, Glenthoj B, Gattaz WF, Moller HJ. 2006. World Federation of Societies of Biological Psychiatry (WFSBP) guidelines for biological treatment of schizophrenia, part 2: long-term treatment of schizophrenia. World J Biol Psychiatry 7:5–40.

Gur RE, Maany V, Mozley PD, Swanson C, Bilker W, Gur RC. 1998. Subcortical MRI volumes in neuroleptic-naive and treated patients with schizophrenia. Am J Psychiatry 155:1711–1717.

Lieberman JA, Tollefson GD, Charles C, et al. 2005. Antipsychotic drug effects on brain morphology in first-episode psychosis. Arch Gen Psychiatry 62:361–370.

Menon V, Anagnoson RT, Glover GH, Pfefferbaum A. 2001. Functional magnetic resonance imaging evidence for disrupted basal ganglia function in schizophrenia. Am J Psychiatry 158:646–649.

Mori T, Ohnishi T, Hashimoto R, et al. 2007. Progressive changes of white matter integrity in schizophrenia revealed by diffusion tensor imaging. Psychiatry Res 154:133–145.

Ohnishi T, Hashimoto R, Mori T, et al. 2006. The association between the Val158Met polymorphism of the catechol-O-methyl transferase gene and morphological abnormalities of the brain in chronic schizophrenia. Brain 129:399–410.

Spinks R, Nopoulos P, Ward J, Fuller R, Magnotta VA, Andreasen NC. 2005. Globus pallidus volume is related to symptom severity in neuroleptic naive patients with schizophrenia. Schizophr Res 73:229–233.

Uranova N, Orlovskaya D, Vikhreva O, et al. 2001. Electron microscopy of oligodendroglia in severe mental illness. Brain Res Bull 55:597–610.

Yoshikawa K, Nakata Y, Yamada K, Nakagawa M. 2004. Early pathological changes in the parkinsonian brain demonstrated by diffusion tensor MRI. J Neurol Neurosurg Psychiatry 75:481–484.

ELSEVIER

NeuroImage

www.elsevier.com/locate/ynimg
NeuroImage 28 (2005) 1014–1021

# The prediction of rapid conversion to Alzheimer's disease in mild cognitive impairment using regional cerebral blood flow SPECT

Kentaro Hirao,[a,e] Takashi Ohnishi,[a,b,*] Yoko Hirata,[a] Fumio Yamashita,[a] Takeyuki Mori,[a] Yoshiya Moriguchi,[a] Hiroshi Matsuda,[a,f] Kiyotaka Nemoto,[a,d] Etsuko Imabayashi,[a,f] Minoru Yamada,[a,f] Toshihiko Iwamoto,[e] Kunimasa Arima,[c] and Takashi Asada[d]

[a]*Department of Radiology, National Center Hospital of Mental, Nervous, and Muscular Disorders, National Center of Neurology and Psychiatry, Tokyo, Japan*
[b]*Department of Investigative Radiology, Research Institute, National Cardiovascular Center, Osaka, Japan*
[c]*Department of Laboratory Medicine, National Center Hospital of Mental, Nervous, and Muscular Disorders, National Center of Neurology and Psychiatry, Tokyo, Japan*
[d]*Department of Psychiatry, Institute of Clinical Medicine, University of Tsukuba, Japan*
[e]*Department of Geriatric Medicine, Tokyo Medical University, Japan*
[f]*Department of Nuclear Medicine, Saitama Medical School, Japan*

Received 13 April 2005; revised 7 June 2005; accepted 30 June 2005
Available online 29 August 2005

**Mild cognitive impairment (MCI) comprises a heterogeneous group with a variety of clinical outcomes and they are at risk for developing Alzheimer's disease (AD). The prediction of conversion from MCI to AD using the initial neuroimaging studies is an important research topic. We investigated the initial regional cerebral blood flow (rCBF) measurements using single photon emission computed tomography (SPECT) in individuals with 76 amnesic MCI (52 subjects converted to AD and 24 subjects did not convert to AD at 3-year follow-up) and 57 age- and gender-matched controls. We sought functional profiles associated with conversion to AD, then evaluated the predictive value of the initial rCBF SPECT. As compared with controls, AD converters demonstrated reduced blood flow in the bilateral parahippocampal gyri, precunei, posterior cingulate cortices, bilateral parietal association areas, and the right middle temporal gyrus. Non-converters also demonstrated significant reduction of rCBF in the posterior cingulated cortices and the right caudate nucleus when compared to controls. As compared with non-converters, converters showed reductions of rCBF in the bilateral temporo-parietal areas and the precunei. The logistic regression model revealed that reduced rCBF in the inferior parietal lobule, angular gyrus, and precunei has high predictive value and discriminative ability. Although a cross-validation study is needed to conclude the usefulness of rCBF SPECT for the prediction of AD conversion in individuals with MCI, our data suggest that the initial rCBF SPECT studies of individuals with MCI may be useful in predicting who will convert to AD in the near future.**


*Keywords:* Mild cognitive impairment (MCI); Alzheimer's disease (AD); Regional cerebral blood flow (rCBF); Single photon emission computed tomography (SPECT)

## Introduction

Mild cognitive impairment (MCI) is an operational diagnostic term developed to describe the preclinical stage of Alzheimer's disease (AD) (Petersen et al., 2001a). The risk for conversion to AD is higher in individuals with MCI than in the general aged population, as annual conversion rate of 6%–25% from MCI to AD (Petersen et al., 2001b). Furthermore, a recent study suggested that progression from MCI to AD is time-dependent. According to Palmer's study, people with MCI have a high risk of progressing to dementia over the next 3 years, and the risk starts to decrease after this point (Palmer et al., 2003). The early detection of MCI individuals who will later convert to AD is an important issue for both clinical and research interests.

The recent advance of computer-assisted statistical image analyses revealed that subjects with very mild AD typically show abnormal metabolic and regional cerebral blood flow (rCBF) patterns, even at the preclinical stage. Using glucose metabolism positron emission tomography (PET) with a voxel-by-voxel statistical analysis, Minoshima et al. reported that the earliest changes observed in very mild AD were in the posterior cingulate cortex (PCC) (Minoshima et al., 1997). This unexpected finding has

* Corresponding author. Department of Radiology, National Center Hospital of Mental, Nervous, and Muscular Disorders, National Center of Neurology and Psychiatry 4-1-1 Ogawa Higashi, Kodaira City, Tokyo 187-0031, Japan.
*E-mail address:* tohnishi@hotmail.com (T. Ohnishi).
**Available online on ScienceDirect (www.sciencedirect.com).**

1053-8119/$ - see front matter © 2005 Elsevier Inc. All rights reserved.
doi:10.1016/j.neuroimage.2005.06.066

been replicated by other groups using both glucose metabolism measurements with PET and even less sophisticated measurement techniques such as regional cerebral blood flow (rCBF) measurements with single photon emission computed tomography (rCBF SPECT). Our previous rCBF SPECT study demonstrated significantly decreased rCBF in the posterior cingulate gyri and precunei bilaterally in MCI subjects as compared with controls at least 2 years before they met a clinical diagnosis of AD (Kogure et al., 2000). We also reported a diagnostic value of reduced rCBF in the posterior cingulate cortex (PCC) to assist in discriminating between normal subjects and MCI subjects who later developed AD (Imabayashi et al., 2004). Furthermore, a PET study demonstrated hypometabolism of the PCC in young subjects with a high genetic risk of developing AD (Reiman et al., 2004). These results suggest that functional neuroimaging techniques such as PET and SPECT may be promising techniques for the preclinical diagnosis of AD.

However, MCI is a heterogeneous diagnostic category comprised of individuals with a variety of clinical outcomes (Petersen et al., 2001). As such, only a longitudinal study comparing MCI subjects who convert to AD at follow-up (converters) with MCI subjects who do not convert at follow-up (non-converters) is appropriate to determine the predictive value of initial neuroimaging for progression of MCI to AD. Only a few longitudinal studies have been published so far (Celsis et al., 1997; Arnaiz et al., 2001; Huang et al., 2002; Chetelat et al., 2003; Drzezga et al., 2003; Mosconi et al., 2004). These studies have suggested that reduced glucose metabolism in the right temporo-parietal cortex or reduced rCBF and glucose metabolism in the PCC might be good predictors of progression to AD.

On the other hand, morphological magnetic resonance imaging (MRI) studies have demonstrated that higher atrophy rates in the medial temporal regions such as the entorhinal cortex and hippocampus may be good predictors of conversion to AD (Jack et al., 1999; Mungas et al., 2002; Nestor et al., 2004). However, such serial MR studies require at least a 1-year follow-up period to predict AD conversion. As with functional imaging studies, the predictive value of morphological MR studies has not been yet clarified.

The present retrospective cohort study assessed initial rCBF SPECT images in a group of amnesic MCI subjects consisting of AD converters and non-converters who were followed clinically for 3 years. The aim of the present study was to find highly specific and sensitive rCBF changes capable of discriminating between MCI subjects who eventually develop AD from those who do not convert to AD, as early as possible. We also demonstrated the predictive value of the initial rCBF SPECT studies in MCI subjects.

## Methods

### *Subjects*

The characteristics of the subjects who participated in this study are summarized in Table 1. We retrospectively studied 82 individuals (40 men and 42 women) with MCI who visited our memory clinic with a chief complaint of memory disturbance. Six MCI subjects (3 men and 3 women) dropped out and therefore their outcomes were unknown. Analyses therefore included 76 MCI subjects (37 men and 39 women) and 57 age- and gender-matched control subjects. All subjects were free of depression as operationalized as a score less than 8 on the Hamilton Depression Scale (Hamilton, 1960). MCI was diagnosed using the criteria proposed by Mayo Clinic Alzheimer's Disease Research Center. Recently, the criteria of MCI was modified (Pertersen, 2004), but when our study was conducted, the criteria required: (1) memory complaint by patient, family, or physician; (2) normal activities of daily living; (3) normal global cognitive function; (4) objective impairment in memory or in one other area of cognitive function as evident by scores >1.5 SD below the age appropriate mean; (5) CDR score (Hughes et al., 1982) of 0.5; and (6) absence of dementia.

MCI subjects ranged in age from 48 to 86 years with a mean ± standard deviation (SD) of 69.0 ± 8.6 years. The Mini-Mental State Examination (MMSE) (Folstein et al., 1975) score ranged from 24 to 29 (mean ± SD 26.5 ± 1.6) at the initial visit. During the subsequent follow-up period of 3 years, 52 patients showed progressive cognitive decline and eventually fulfilled the diagnosis

Table 1
The characteristics of subjects

| | MCI (M:F = 37:39) | | | Results of ANOVA | |
|---|---|---|---|---|---|
| | Controls (M:F = 30:27) | Non-converters (M:F = 12:12) | Converters (M:F = 25:27) | *F* value | *P* value |
| Age | 70.4 ± 7.3 | 68.7 ± 7.6 | 69.2 ± 9.1 | 0.5 | 0.6 |
| Education in years | 12.2 ± 2.9 | 12.2 ± 3.1 | 12.0 ± 3.1 | 0.1 | 0.9 |
| MMSE | 28.8 ± 1.5 | 27.0 ± 1.3* | 26.2 ± 1.7* | 38.7 | <0.001 |
| MMSE (about after 3 years) | | 26.1 ± 1.4* | 19.1 ± 4.3****** | 126.1 | <0.001 |
| Digit span | | | | | |
| Forward | 5.3 ± 1.0 | 5.6 ± 1.0 | 5.4 ± 1.0 | 0.5 | 0.6 |
| Backward | 4.1 ± 0.8 | 4.2 ± 0.8 | 4.1 ± 1.0 | 0.2 | 0.8 |
| List learning (10 words) | | | | | |
| Delayed recall (30 min) | 7.9 ± 1.2 | 3.7 ± 3.6* | 0.9 ± 2.0****** | 117 | <0.001 |
| Story recall (15 elements) | | | | | |
| Delayed (30 min) | 7.9 ± 2.5 | 0.87 ± 1.72* | 0.9 ± 1.72* | 101.8 | <0.001 |
| Rey–Osterrieth complex figure test | | | | | |
| Delayed recall (30 min) | 14.47 ± 6.31 | 4.28 ± 3.76* | 2.9 ± 6.93*** | 85.3 | <0.001 |

*Note.* Data are mean ± SD in controls ($n$ = 57) or MCI ($n$ = 76).

* Scores of MCI are significantly lower than those of controls. $P < 0.05$ (Bonferroni correction for multiple comparison).

** Scores of the converters are significantly lower than those of non-converters, $P < 0.05$ (Bonferroni correction for multiple comparison).

*** Scores of the converters are significantly lower than those of non-converters. $P < 0.001$ (Bonferroni correction for multiple independent comparisons).

**** Scores of the follow up MMSE are significantly lower than those of the initial MMSE, $P < 0.05$ (paired $t$ test).

of probable AD according to the National Institute of Neurologic and Communicative Disorders and Stroke and the Alzheimer's Disease and Related Disorders Association criteria (NINCDS-ADRDA) (McKhann et al., 1984). Twenty-four of the 76 MCI subjects still did not fulfill the criteria for dementia according to DSM-IV (American Psychiatric Association, 1994) during the follow-up period. Of these participants, 40 converters and 12 non-converters completed follow-up rCBF SPECT studies at the end of the 3-year follow-up period.

Fifty-seven individuals (30 men and 27 women; age 56–86 years, mean ± SD 70.4 ± 7.3 years) did not have memory impairment or cognitive disorders and were assigned to the normal control group. Specifically, their performances were within normal limits (<1 SD) both on the Wechsler Memory Scale-Revised and on the Wechsler Adult Intelligence Scale-Revised, and their MMSE score ranged from 25 to 30 (mean ± SD 28.8 ± 1.5). None of these control subjects manifested cognitive changes during the follow-up period of more than 3 years. The control group did not differ significantly in age or education from the MCI group.

The local ethics committee approved this study for both healthy volunteers and MCI subjects, all of whom gave their informed consent to participate. All subjects were right-handed and screened by questionnaire regarding medical history and excluded if they had neurological, psychiatric, or medical conditions that could potentially affect the central nervous system, such as substance abuse or dependence, atypical headache, head trauma with loss of consciousness, asymptomatic or symptomatic cerebral infarction detected by T2-weighted MRI, hypertension, chronic lung disease, kidney disease, chronic hepatic disease, cancer, or diabetes mellitus.

### *SPECT imaging*

Before the SPECT scan was performed, all subjects had an intravenous line established. They were injected while lying supine with eyes closed in a dimly lit quiet room. Each subject received an intravenous injection of 600 MBq of technetium-99 m ethyl cysteinate dimer (99 mTc-ECD). Ten minutes after the injection of 99 mTc-ECD, brain SPECT was performed using three-head rotating gamma cameras (Multispect3; Siemens Medical Systems, Inc., Hoffman Estates, IL) equipped with high-resolution fan-beam collimators. For each camera, projection data were obtained in a 128 × 128 format for 24 angles at 50 s per angle. A Shepp and Logan Hanning filter was used for SPECT image reconstruction at 0.7 cycle/cm. Attenuation correction was performed using Chang's method.

### *Statistical parametric mapping*

Images were analyzed with the statistical parametric mapping software SPM99 (Wellcome Department of Cognitive Neurology, UK). Using a template for Tc-99 m ECD template, the SPECT data were transformed into a standard stereotaxic space (MNI). The spatial normalization algorithm of SPM99 was used for linear and non-linear transformation (basis function: 8 × 9 × 8; iteration: 16). A Gaussian filter (12 mm full width at half maximum) was used to smooth each image. The effect of global differences in CBF between scans was removed by proportional scaling with the threshold at 60% of whole brain activity. Using MRIcro (www.mricro.com), we checked the mask image for statistical analysis and verified that medial temporal regions including the parahippocampal gyrus and hippocampus were encompassed in the analysis. To test hypotheses about regional population effects, data were analyzed by analysis of variance (ANOVA) using the full monthly option. For this $F$ test, we used an alpha value of 0.001 as our level of significance to correct for multiple comparisons. Group comparisons were also done using $t$ tests within the ANOVA design matrix (uncorrected $P < 0.001$ and cluster extent $K > 100$ voxels, small volume correction (SVC) for correction of multiple comparisons). There were twice as many converters as non-converters raising the concern that the SPECT abnormalities in the former might be influenced by statistical power. Therefore, we randomly subdivided AD converters into 2 groups where the group size was matched to that of non-converters. Then, two-sample $t$ tests between non-converters and each group of AD converters were done (uncorrected $P < 0.001$). The resulting sets of $t$ values constituted the statistical parametric maps {SPM ($t$)}. Anatomic localization was identified using both MNI coordinates and Talairach coordinates obtained from M. Brett's transformations (http://www.mrc-cbu.cam.ac.uk/Imaging/mnispace.html) and were presented as Talairach coordinates (Talairach and Tournoux, 1988).

### *Logistic regression model*

To evaluate the predictive value of rCBF change observed in the initial rCBF SPECT, we used as independent variables (X1) $Z$ scores for the mean adjusted rCBF value at the significant clusters obtained from the SPM ($t$) map in the group comparison (AD converter vs. Non-converter) for the logistic regression model:

$$Y = b0 + b1*X1$$

where $Y$ is the logit transformation of the probability $P$. The logit transformation of the probability of a value is defined as:

$$Y = \log(P/(1-P))$$

where $P$ is the probability of conversion from MCI to AD.

The mean value of the adjusted rCBF in each cluster of each subject was extracted using the Marsbar program (http://www.marsbar.sourceforge.net/), then the $Z$ score was calculated using the following formula: $Z$ score = (mean adjusted rCBF value in the control group minus individual value of adjusted rCBF value)/SD of rCBF value in the control group. The logistic regression model analysis was performed using Statistical Package for the Social Sciences (SPSS, Japan Co., Tokyo, Japan). Because the neuropsychological test scores of converters were significantly lower than those of non-converters (especially on delayed recall of list learning and delayed recall of Rey–Osterrieth Complex Figure Test), we also evaluated the predictive value of those scores at the initial visit using logistic regression analysis.

## Results

### *Conversion rate*

In our study, 52 of 82 individuals with MCI converted to AD during the 3-year follow-up period. The annual conversion rate of MCI to AD was approximately 21.14%.

*Group comparisons*

The ANOVA analysis [SPM ($F$), $P < 0.001$, corrected for multiple comparisons with family-wise alpha < 0.05] revealed a significant difference among groups in the bilateral precunei (Brodmann area [BA] 7), the posterior cingulate cortices (PCC, BA31, peak $x, y, z = 0, -47, 32$, $F$ value = 35.93), the right inferior parietal lobule (BA40, peak $x, y, z = 46, -64, 44$, $F$ value = 25.23) and the left angular gyrus (BA39, peak $x, y, z = -42, -60, 38$, $F$ value = 16.77) (Fig. 1a). In comparison with controls, AD converters demonstrated reduced blood flow in the bilateral parahippocampal gyri, precunei, PCC, bilateral parietal association areas, and the right middle temporal gyrus (Fig. 1b, Table 2). Non-converters also demonstrated significant reduction of rCBF in the PCC and the right caudate nucleus when compared to controls (Fig. 1c, Table 2). Importantly, significant differences in the bilateral precunei and parietal association areas were found between converters and non-converters (Fig. 1d, Table 2).

*Group comparisons of subdivided groups of converters and the non-converters*

As compared to non-converters, the first group of 26 converters showed significantly decreased rCBF in the right inferior parietal lobule (Talairach coordinate: 46, −64, 47, $t$ value: 3.82, cluster size: 115) and the left angular gyrus (Talairach coordinate: −40, −58, 36, $t$ value: 4.45, cluster size: 127) (Fig. 2 left). The essentially same result was found in the comparison between non-converters and the second group of 26 converters (Right IPL: Talairach coordinate: 53, −58, 42, $t$ value: 3.65, cluster size: 44; Left angular gyrus: Talairach coordinate: −40, −57, 34, $t$ value: 4.81, cluster size: 180) (Fig. 2, right). We could not find reduced rCBF in the precunei at $P < 0.001$; however, reduction in the precunei was detected at a lenient statistical threshold ($P < 0.005$ without multiple comparisons) in each group comparison (data were not shown).

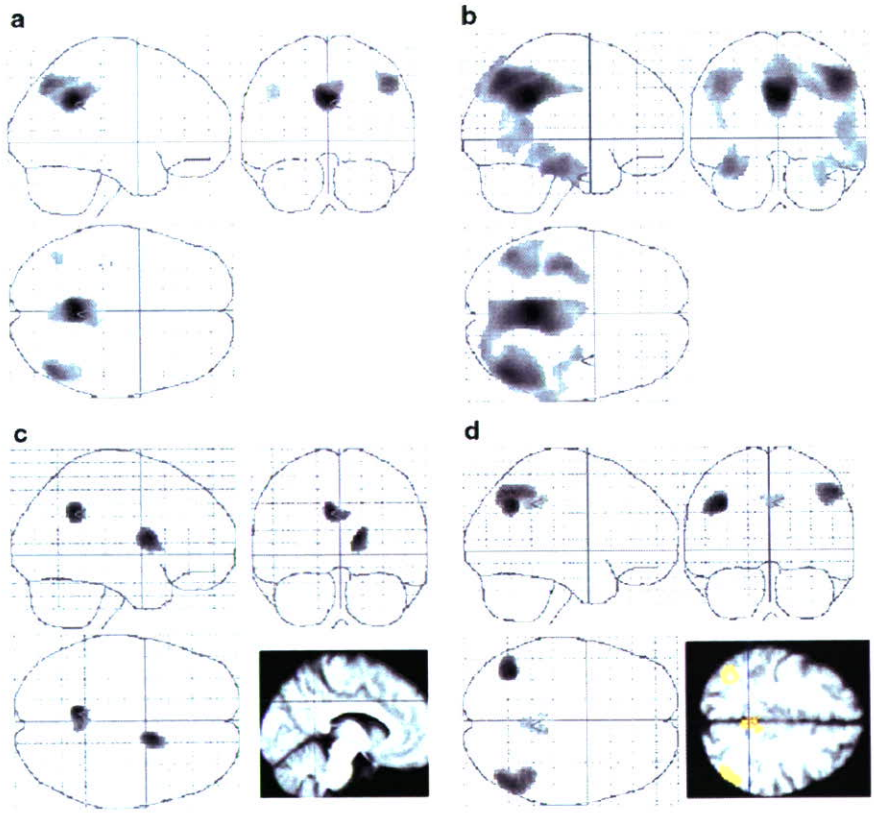


Fig. 1. Results of group comparisons. (a) The SPM {$F$} is displayed in a standard format as a maximum-intensity projection viewed from the right, the back, and the top of the brain. The anatomical space corresponds to the atlas of Talairach and Tournoux. Representation in stereotaxic space of regions with significantly differences between groups (corrected $P < 0.05$) was demonstrated. The ANOVA demonstrated a significant difference among groups in the bilateral precunei, the posterior cingulate cortices, the right inferior parietal lobule, and the left angular gyrus. (b) The SPM is displayed in a standard format as a maximum-intensity projection of regions with significantly decreased rCBF in converters compared with the control group [$P < 0.001$, corrected by small volume correction (SVC)]. The converters demonstrated reduced blood flow in the bilateral parahippocampal gyri, precunei, PCC, bilateral parietal association areas, and the right middle temporal gyrus. (c) The SPM is displayed in a standard format as a maximum-intensity projection of regions with significantly decreased rCBF in non-converters compared with the control group ($P < 0.001$, corrected by SVC). Non-converters demonstrated significant reduction of rCBF in the PCC and the right caudate nucleus. (d) The SPM is displayed in a standard format as a maximum-intensity projection of regions with significantly decreased rCBF in converters compared with non-converters ($P < 0.001$, corrected by SVC). The converters showed a significant reduction of rCBF in the bilateral precunei and parietal association areas.

Table 2
Results of group comparisons and paired $t$ tests

| Region | BA | Coordinates | | | $K$ | Corrected $P$ value (with small volume correction) | $t$ value |
|---|---|---|---|---|---|---|---|
| | | $x$ | $y$ | $z$ | | | |
| *Controls > AD converters* | | | | | | | |
| Bilateral precuneus, and PCC | BA31 | | | | | | |
| | B7 | 2 | −45 | 32 | 6794 | <0.001 | 8.46 |
| R IPL | BA40 | 46 | −64 | 44 | 6794 | <0.001 | 6.95 |
| L Angular gyrus, IPL | BA39 | −42 | −60 | 38 | 1301 | <0.001 | 5.24 |
| L PHG | BA20,36 | −38 | −22 | −17 | 771 | <0.001 | 5.36 |
| R PHG | BA20,36 | 34 | −15 | −19 | 535 | 0.005 | 3.97 |
| R Middle temporal gyrus | BA21 | 63 | −37 | −8 | 535 | 0.008 | 4.25 |
| *Controls > MCI non-converters* | | | | | | | |
| L PCC | BA31 | −8 | −49 | 34 | 231 | <0.001 | 4.83 |
| R PCC | BA31 | 4 | −47 | 30 | 231 | 0.003 | 3.81 |
| R Caudate nucleus | | 14 | 6 | 11 | 158 | <0.001 | 4.63 |
| *MCI non-converters > AD converters* | | | | | | | |
| R IPL | BA40 | 51 | −58 | 45 | 653 | 0.001 | 4.49 |
| L Angular gyrus | BA39 | −38 | −58 | 36 | 368 | <0.001 | 5.21 |
| L Precuneus | BA7 | −6 | −35 | 42 | 140 | 0.014 | 3.34 |
| R Precuneus | BA7 | 2 | −45 | 43 | 140 | 0.009 | 3.51 |

BA: Brodmann area, IPL: inferior parietal lobule, PCC: posterior cingulate cortex, PHG: Parahippocampal gyrus.

*The predictive value of rCBF changes observed at initial SPECT and scores of neuropsychological tests*

Given the results of the group comparisons, we hypothesized that rCBF changes in the precuneus and the parietal association areas would be good predictors of progression from MCI to AD in individuals with MCI. Using the $Z$ score of each region (Fig. 3) for each MCI subject, we determined the predictive value of the initial rCBF SPECT using a logistic regression analysis. Table 3 shows the results of the logistic regression analysis. We found that higher $Z$ scores in the left angular area (Wald $\chi^2 = 11.1$, $df = 1$, $P = 0.001$, odds ratio [OR] 2.174, 95% confidence interval [CI] = 1.38–3.43), right inferior parietal lobule (Wald $\chi^2 = 10.7$, $df = 1$, $P = 0.001$, OR 2.13, 95% CI = 1.35–3.35), and the precuneus (Wald $\chi^2 = 10.13$, $df = 1$, $P = 0.001$, OR 2.417, 95% CI = 1.4–4.16) were good predictors of progression from MCI to AD (Table 3). A cutoff value of 0.5, which best divided the converter and non-converters, provided high sensitivity (82–90%) and adequate overall accuracy (68–73%) in each region (Table 3).

In contrast, lower scores on delayed recall of list learning (Wald $\chi^2 = 8.369$, $df = 1$, $P = 0.004$, odds ratio [OR] 1.413, 95% confidence interval [CI] = 1.118–1.786) and lower scores on delayed recall of the Rey–Osterrieth Complex Figure Test (ROCFT) (Wald $\chi^2 = 7.092$, $df = 1$, $P = 0.008$, OR 1.167, 95% CI = 1.042–1.308) had lower predictive values than those of the rCBF changes observed in SPECT studies. A cutoff value of 0.5, which best divided the converters and non-converters, revealed similar sensitivity (90.3% for word leaning and 86.2% for ROCFT,

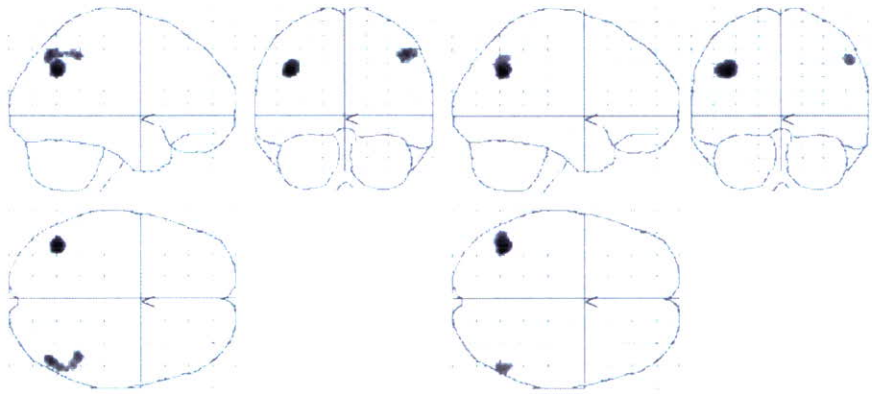

Fig. 2. Results of group comparisons of subdivided groups of converters and the non-converters. The SPM is displayed in a standard format as MIP of regions with significantly decreased in rCBF in converters compared with non-converters (uncorrected $P < 0.001$). Fifty-two converters were randomly divided two groups. Then, two-sample $t$ tests between non-converters and each group of AD converters were done. Left: The first group of converters showed a significantly decreased rCBF in the left angular gyrus and the right inferior parietal lobule. Right: The second group of converters also showed essentially the same result.

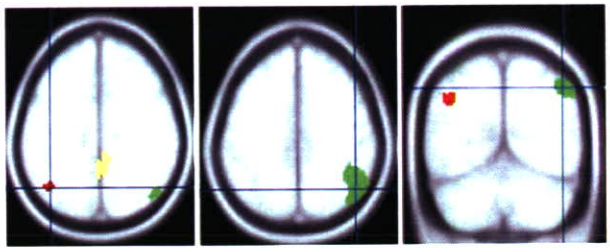

Fig. 3. Regions of interest (ROIs) for the logistic regression model. Red: The ROI for the *Z* score in the left angular gyrus. Yellow: The ROI for the *Z* score in the bilateral precunei. Green: The ROI for the *Z* score in the right inferior parietal lobule.

respectively) and overall accuracy (69.8% for word leaning and 78% for ROCFT respectively) to the sensitivity and accuracy associated with the rCBF changes observed in the initial SPECT (Table 3).

## Discussion

### *The conversion rate*

The annual conversion rate of MCI to AD in the current study was 21.14%, which is higher than that observed in other cohorts of MCI subjects (Bruscoli and Lovestone, 2004). A recent review of conversion studies reported that the overall rate of conversion was 10%, but that large differences existed between studies (Bruscoli and Lovestone, 2004). The single most important variable accounting for between-study heterogeneity was the source of subjects, with self-selected clinic attendees having the highest conversion rate (Bruscoli and Lovestone, 2004). In our study, all individuals with MCI were outpatients that attended a memory clinic, and therefore the high conversion rate in the study is not surprising.

### *Different rCBF changes between converters and non-converters and the predictive value of initial SPECT study*

In this study, converters displayed a significant reduction of rCBF in the precuneus and bilateral parietal association areas when compared to non-converters. Although the sample size of converters was larger than that of non-converters, the results of group comparisons with randomly re-sampling the converters in cohorts where the sample sizes were matched to that of non-converters demonstrated essentially the same results. The fact indicated that the greater extent of rCBF abnormalities in converters was not influenced by statistical power. Importantly, we also found that reduction of rCBF in these areas is a good predictor of conversion from MCI to AD. Performance on measures of delayed recall of word learning and ROCFT also showed relatively high discriminative ability, although these scores had lower odds ratios than those associated with reduction of rCBF. These results demonstrate the utility of rCBF SPECT for the prediction of AD conversion. Previous functional neuroimaging studies in very early AD and MCI have consistently demonstrated dysfunction in the PCC and cinguloparietal transitional area or precuneus (Minoshima et al., 1997; Kogure et al., 2000; Imabayashi et al., 2004). A recent PET study showed that the retrosplenial PCC was the only abnormality common to all MCI individuals (Nestor et al., 2003a,b). However, our data suggest that reduced rCBF in the parietal association areas and precuneus are better predictors than PCC hypoperfusion. Indeed, the comparison between the controls and non-converters also demonstrated a significant reduction of rCBF in the PCC. We consider that hypoperfusion in the temporo-parietal regions could be more advanced signs of AD pathology and may precede manifestation of clinical symptoms of AD, and therefore they were better predictors of early conversion. A recent longitudinal FDG-PET study reported similar results to those of the present study: a high predictive value of reduced FDG uptake in the parietal association areas and a lower predictive value of that in the PCC (Chetelat et al., 2003). Mosconi et al. also reported that converters demonstrated reduced glucose metabolism in the inferior parietal cortex as compared with non-converters (Mosconi et al., 2004). Although Nestor's study emphasized the importance of functional abnormality of the retrosplenial cortex in MCI subjects, they also reported that MCI subjects with additional hypometabolism in the parietal association areas converted to AD during the follow-up period (Nestor et al., 2003). These results in conjunction with the current results strongly demonstrate the high predictive value of functional abnormality in the parietal association areas. Furthermore, these results are consistent with the results of a postmortem study of tau pathology in aging and AD (Delacourte et al., 1999). According to Delacourte's study, neurofibrillary degeneration (NFD) with paired helical filaments (PHF)-tau was systematically present in varying amounts in the hippocampal region of non-demented aged subjects, whereas tau pathology in the angular gyrus (BA39) and dorsolateral prefrontal cortex (BA9) was found in all AD patients

Table 3
Results of logistic regression model

| | Odds ratio | 95% CI | *P* value | Sensitivity (%) | Overall accuracy (%) |
|---|---|---|---|---|---|
| *SPECT imaging test* | | | | | |
| Regions | | | | | |
| L Angular gyrus | 2.174 | 1.38–3.43 | <0.001 | 82 | 68 |
| R IPL | 2.130 | 1.35–3.35 | <0.001 | 90 | 73.3 |
| Precuneus | 2.417 | 1.40–4.161 | <0.001 | 88 | 73.3 |
| *Neuropsychological test* | | | | | |
| List learning (delayed recall) | 1.413 | 1.118–1.786 | 0.004 | 90.3 | 69.8 |
| Rey–Osterrieth complex figure test (delayed recall) | 1.167 | 1.042–1.308 | 0.008 | 86.2 | 78 |

CI: confidence interval, IPL: inferior parietal lobule.

(Delacourte et al., 1999). The data support the notion that functional abnormality in the parietal association areas should be a *better predictor* of AD conversion. However, two longitudinal studies (Huang et al., 2002; Drzezga et al., 2003) suggested high predictive value of functional abnormality in the PCC; further study will be needed to clarify the predictive value of the functional abnormality in the PCC.

Unexpectedly, we found decreased rCBF in the right caudate nucleus in comparing controls and non-converters. A recent voxel-based volumetric MR study (Frisoni et al., 2002) revealed reduced gray matter volume of caudate nucleus in mild AD; however, we have no good explanation or hypothesis about this finding at the present moment.

### *Reduction of rCBF in the parahippocampal gyrus in converters*

In this study, we found reduced parahippocampal rCBF in converters. Numerous structural MRI studies have demonstrated that progressive atrophy of the parahippocampal area including the entorhinal cortex is a sensitive marker for detecting and predicting AD (Chetelat and Baron, 2003; Korf et al., 2004; Nestor et al., 2004). In this study, we did not apply a partial volume effect (PVE) correction for SPECT imaging; therefore, one could argue that reduced rCBF in the parahippocampal area could be explained by partial volume effect. We agree that PVE partially contributes to the results of our study. However, an atrophy-corrected FDG-PET study demonstrated hippocampal hypometabolism in AD and MCI and the study's authors concluded that metabolism reductions exceed volume losses in MCI (De Santi et al., 2001). Other studies with MRI-guided FDG-PET also demonstrated hypometabolism of the limbic systems (de Leon et al., 2001; Nestor et al., 2003a,b) including the entorhinal cortex in MCI.

### *Limitations of this study*

The first limitation of this study is that we did not evaluate the cross-validity of the predictive value of the SPECT findings using split-half reliability due to the limited number of non-converters. To conclude the usefulness of rCBF SPECT in predicting AD conversion, our data should be replicated in other cohorts. In this context, our data may be considered to be preliminary rather than conclusive. However, other studies conducted by different research groups using a different imaging method (FDG-PET) reported similar results to those of the present study (Chetelat et al., 2003), and we believe that our predictive model should be reliable.

Second, we did not perform the correction of partial volume effects (PVE) for SPECT images. We agree that PVE could partially contribute to the results of the present study. Even so, the predictive value of rCBF patterns identified in this study still has diagnostic value. From a diagnostic point of view, atrophy-related hypoperfusion is a consequence of AD pathology and might improve the detection of early functional abnormalities.

Finally, some may argue that a 3-year follow-up is not long enough. We agree that it remains a possibility that some of the non-converters would develop AD during a longer observation period, because the logistic model cannot be certain that someone will not convert AD after the follow-up period. However, we can still distinguish rapid converters from slow converters or slow decliners using the initial SPECT study. The results suggest that the initial SPECT study can discriminate between rapid decliners and slow decliners. Such discrimination is important for both therapeutic and research purposes.

## Conclusion

We demonstrated that the rCBF reductions in the parietal association areas and the precunei are a good predictor of progression from MCI to AD. The data suggest that the initial rCBF SPECT in individuals with MCI could be a promising method to accurately predict who would meet diagnostic criteria for AD in the next 3 years.

## Acknowledgment

This study was supported by the Promotion of Fundamental Studies in Health Science of Organization for Pharmaceuticals and Medical Devices Agency.

## References

American Psychiatric Association, 1994. Diagnostic and Statistical Manual of Mental Disorders. DSM-IV (4th ed.). American Psychiatric Association, Washington, DC.

Arnaiz, E., Jelic, V., Almkvist, O., Wahlund, L.O., Winblad, B., Valind, S., et al., 2001. Impaired cerebral glucose metabolism and cognitive functioning predict deterioration in mild cognitive impairment. NeuroReport 12, 851–855.

Bruscoli, M., Lovestone, S., 2004. Is MCI really just early dementia? A systematic review of conversion studies. Int. Psychogeriatr. 16, 129–140.

Celsis, P., Agniel, A., Cardebat, D., Demonet, J.F., Ousset, P.J., Puel, M., 1997. Age related cognitive decline: a clinical entity? A longitudinal study of cerebral blood flow and memory performance. J. Neurol. Neurosurg. Psychiatry 62, 601–608.

Chetelat, G., Baron, J.C., 2003. Early diagnosis of Alzheimer's disease: contribution of structural neuroimaging. NeuroImage 18, 525–541.

Chetelat, G., Desgranges, B., de la Sayette, V., Viader, F., Eustache, F., Baron, J.C., 2003. Mild cognitive impairment: can FDG-PET predict who is to rapidly convert to Alzheimer's disease? Neurology 60, 1374–1377.

de Leon, M.J., Convit, A., Wolf, O.T., Tarshish, C.Y., DeSanti, S., Rusinek, H., et al., 2001. Prediction of cognitive decline in normal elderly subjects with 2-[(18)F]fluoro-2-deoxy-D-glucose/poitron-emission tomography (FDG/PET). Proc. Natl. Acad. Sci. U. S. A. 98, 10966–10971.

De Santi, S., de Leon, M.J., Rusinek, H., Convit, A., Tarshish, C.Y., Roche, A., et al., 2001. Hippocampal formation glucose metabolism and volume losses in MCI and AD. Neurobiol. Aging 22, 529–539.

Delacourte, A., David, J.P., Sergeant, N., Buee, L., Wattez, A., Vermersch, P., et al., 1999. The biochemical pathway of neurofibrillary degeneration in aging and Alzheimer's disease. Neurology 52, 1158–1165.

Drzezga, A., Lautenschlager, N., Siebner, H., Riemenschneider, M., Willoch, F., Minoshima, S., et al., 2003. Cerebral metabolic changes accompanying conversion of mild cognitive impairment into Alzheimer's disease: a PET follow-up study. Eur. J. Nucl. Med. Mol. Imaging 30, 1104–1113.

Folstein, M.F., Folstein, S.E., McHugh, P.R., 1975. "Mini-mental state". A practical method for grading the cognitive state of patients for the clinician. J. Psychiatr. Res. 12, 189–198.

Frisoni, G.B., Testa, C., Zorzan, A., Sabattoli, F., Beltramello, A., Soininen, H., et al., 2002. Detection of grey matter loss in mild Alzheimer's disease with voxel based morphometry. J. Neurol. Neurosurg. Psychiatry. 73, 657–664.

Hamilton, M., 1960. A rating scale for depression. J. Neurol. Neurosurg. Psychiatry 23, 56–62.

Huang, C., Wahlund, L.O., Svensson, L., Winblad, B., Julin, P., 2002. Cingulate cortex hypoperfusion predicts Alzheimer's disease in mild cognitive impairment. BMC Neurol. 2, 9.

Hughes, C.P., Berg, L., Danziger, W.L., Coben, L.A., Martin, R.L., 1982. A new clinical scale for the staging of dementia. Br. J. Psychiatry 140, 566–572.

Imabayashi, E., Matsuda, H., Asada, T., Ohnishi, T., Sakamoto, S., Nakano, S., et al., 2004. Superiority of 3-dimensional stereotactic surface projection analysis over visual inspection in discrimination of patients with very early Alzheimer's disease from controls using brain perfusion SPECT. J. Nucl. Med. 45, 1450–1457.

Jack Jr., C.R., Petersen, R.C., Xu, Y.C., O'Brien, P.C., Smith, G.E., Ivnik, R.J., 1999. Prediction of AD with MRI-based hippocampal volume in mild cognitive impairment. Neurology 52, 1397–1403.

Kogure, D., Matsuda, H., Ohnishi, T., Asada, T., Uno, M., Kunihiro, T., et al., 2000. Longitudinal evaluation of early Alzheimer's disease using brain perfusion SPECT. J. Nucl. Med. 41, 1155–1162.

Korf, E.S., Wahlund, L.O., Visser, P.J., Scheltens, P., 2004. Medial temporal lobe atrophy on MRI predicts dementia in patients with mild cognitive impairment. Neurology 63, 94–100.

McKhann, G., Drachman, D., Folstein, M., Katzman, R., Price, D., Stadlan, E.M., 1984. Clinical diagnosis of Alzheimer's disease: report of the NINCDS-ADRDA Work Group under the auspices of Department of Health and Human Services Task Force on Alzheimer's Disease. Neurology 34, 939–944.

Minoshima, S., Giordani, B., Berent, S., Frey, K.A., Foster, N.L., Kuhl, D.E., 1997. Metabolic reduction in the posterior cingulate cortex in very early Alzheimer's disease. Ann. Neurol. 42, 85–94.

Mosconi, L., Perani, D., Sorbi, S., Herholz, K., Nacmias, B., Holthoff, V., Salmon, E., Baron, J.C., De Cristofaro, M.T., Padovani, A., Borroni, B., Franceschi, M., Bracco, L., Pupi, A., 2004. MCI conversion to dementia and the APOE genotype: a prediction study with FDG-PET. Neurology 63, 2332–2340.

Mungas, D., Reed, B.R., Jagust, W.J., DeCarli, C., Mack, W.J., Kramer, J.H., et al., 2002. Volumetric MRI predicts rate of cognitive decline related to AD and cerebrovascular disease. Neurology 59, 867–873.

Nestor, P.J., Fryer, T.D., Ikeda, M., Hodges, J.R., 2003a. Retrosplenial cortex (BA 29/30) hypometabolism in mild cognitive impairment (prodromal Alzheimer's disease). Eur. J. Neurosci. 18, 2663–2667.

Nestor, P.J., Fryer, T.D., Smielewski, P., Hodges, J.R., 2003b. Limbic hypometabolism in Alzheimer's disease and mild cognitive impairment. Ann. Neurol. 54, 343–351.

Nestor, P.J., Scheltens, P., Hodges, J.R., 2004. Advances in the early detection of Alzheimer's disease. Nat. Med. 10, S34–S41 (Suppl.).

Palmer, K., Fratiglioni, L., Winblad, B., 2003. What is mild cognitive impairment? Variations in definitions and evolution of nondemented persons with cognitive impairment. Acta Neurol. Scand., Suppl. 179, 14–20.

Petersen, R.C., Doody, R., Kurz, A., Mohs, R.C., Morris, J.C., Rabins, P.V., et al., 2001a. Current concepts in mild cognitive impairment. Arch. Neurol. 58, 1985–1992.

Petersen, R.C., Stevens, J.C., Ganguli, M., Tangalos, E.G., Cummings, J.L., DeKosky, S.T., 2001b. Practice parameter: early detection of dementia: mild cognitive impairment (an evidence-based review). Report of the Quality Standards Subcommittee of the American Academy of Neurology. Neurology 56, 1133–1142.

Reiman, E.M., Chen, K., Alexander, G.E., Caselli, R.J., Bandy, D., Osborne, D., et al., 2004. Functional brain abnormalities in young adults at genetic risk for late-onset Alzheimer's dementia. Proc. Natl. Acad. Sci. U. S. A. 101, 284–289.

Talairach, J., Tournoux, P., 1988. Co-planar Stereotaxic Atlas of the Human Brain. Thieme, Stuttgart.

Available online at www.sciencedirect.com
SCIENCE DIRECT
Neuroscience Research 55 (2006) 361–369
Neuroscience Research
www.elsevier.com/locate/neures

# Navigation ability dependent neural activation in the human brain: An fMRI study

Takashi Ohnishi [a,*], Hiroshi Matsuda [a], Makiko Hirakata [a], Yoshikazu Ugawa [b]

[a] *Department of Radiology, National Center Hospital of Mental, Nervous and Muscular Disorders, National Center of Neurology and Psychiatry, 4-1-1 Ogawa Higashi, Kodaira City, Tokyo 187-8551, Japan*
[b] *Department of Neurology, Division of Neuroscience, Graduate School of Medicine, University of Tokyo, 7-3-1 Hongo, Bunkyo-ku, Tokyo 113-8655, Japan*

Received 30 December 2005; accepted 7 April 2006
Available online 2 June 2006

**Abstract**

Visual-spatial navigation in familiar and unfamiliar environments is an essential requirement of daily life. Animal studies indicated the importance of the hippocampus for navigation. Neuroimaging studies demonstrated gender difference or strategies dependent difference of neural substrates for navigation. Using functional magnetic resonance imaging, we measured brain activity related to navigation in four groups of normal volunteers: good navigators (males and females) and poor navigators (males and females). In a whole group analysis, task related activity was noted in the hippocampus, parahippocampal gyrus, posterior cingulate cortex, precuneus, parietal association areas, and the visual association areas. In group comparisons, good navigators showed a stronger activation in the medial temporal area and precuneus than poor navigators. There was neither sex effect nor interaction effect between sex and navigation ability. The activity in the left medial temporal areas was positively correlated with task performance, whereas activity in the right parietal area was negatively correlated with task performance. Furthermore, the activity in the bilateral medial temporal areas was positively correlated with scores reflecting preferred navigation strategies, whereas activity in the bilateral superior parietal lobules was negatively correlated with them. Our data suggest that different brain activities related to navigation should reflect navigation skill and strategies.


*Keywords:* Functional magnetic resonance imaging; Visual-spatial navigation; Gender difference; Hippocampus; Parietal cortex

## 1. Introduction

Visual-spatial navigation in familiar and unfamiliar environments is an essential requirement of daily life. Several animal studies indicated the importance of the medial temporal lobe, including the hippocampus (place cell) for navigation (O'Keefe and Nadel, 1978; Muller et al., 1987; Eichenbaum et al., 1999). The cognitive-mapping hypothesis suggested a single allocentric (world-centered) representation of the environment residing mainly in the hippocampus proper (O'Keefe and Nadel, 1978), whereas the parietal association areas have been considered to be involved in the egocentric (body-centered) representation in the environment (Colby, 1999). Visual-spatial navigation is a cognitive function in which a reliable sex-specific difference is well known (Galea and Kimura, 1993; Astur et al., 1998; Moffat et al., 1998). A previous functional magnetic resonance imaging human study demonstrated a similar gender-different brain activity associated with a maze navigation task, distinct activation of the left hippocampus in males, whereas females recruited right parietal and right prefrontal cortex (Gron et al., 2000). The results indicated that behavioral gender differences in navigation performance could be accounted for within the framework of different neural substrates for navigation (Gron et al., 2000). However, it has been still unclear whether such a different activation pattern still present even when behavioral performance was controlled. As indicated by psychological studies, there are sex differences in preferred strategies (the route strategy or the orientation strategy) on navigation and acquisition of environmental knowledge (Lawton, 1994, 1996). It would be possible that the different brain activity for navigation may reflect different performance and/or strategies on navigation. In fact, a previous

* Corresponding author. Tel.: +81 42 341 2711; fax: +81 42 346 1790.
*E-mail address:* tohnishi@hotmail.com (T. Ohnishi).

0168-0102/$ – see front matter 
doi:10.1016/j.neures.2006.04.009

fMRI study demonstrated that human subjects spontaneously adopted different strategies to solve a navigation task and these strategies lead to differential activity in the brain (Iaria et al., 2003; Jordan et al., 2004).

To clarify whether distinct functional anatomy of visual-spatial navigation is possibly related to navigation ability, we performed fMRI studies with virtual maze navigation task in four groups of normal subjects consisting of men with a poor navigation ability, men with a good navigation ability, women with a poor navigation ability, and women with a good s navigation ability, and compared brain activities related to a navigation task.

## 2. Methods

### 2.1. Subjects

First as a screening, we asked 246 subjects (133 males: mean age (S.D.) = 30.2 (9.6); 113 females: mean age (S.D.) = 29.8 (13.5)) to fill out a self-administrated questionnaire, the sense of direction questionnaire-short form (SDQ-S) (Takeuchi, 1992). This consists of the following 17 questions pertaining to the sense of direction and comprising two scales, awareness of orientation (nine items) and memory for spatial behavior (eight items). (1) I can make correct choices as to cardinal directions in an unfamiliar place. (2) I have become confused, as to cardinal directions, when I am in an unfamiliar place. (3) I have difficulties in identifying the moving direction of the train with regard to cardinal direction. (4) When I get route information, I can make use of "left or right" information, but I cannot use cardinal directions. (5) I cannot make out which direction my room in a hotel faces. (6) I can tell where I am on a map. (7) I can visualize the route as a map-like image. (8) I feel anxious about my walking direction in an unfamiliar area. (9) I have poor memory for landmarks. (10) I cannot remember landmarks found in an area where I have often been. (11) I cannot use landmarks in finding my way. (12) I cannot remember the different aspects of scenery. (13) I often cannot find the way even if given detailed verbal information regarding the route. (14) I have a lot of difficulties reaching an unknown place even after consulting a map. (15) I often (or easily) forget which direction I turned. (16) I become totally confused as to the correct sequence of the return way as a consequence of a number of left–right turns in the route. (17) I cannot verify landmarks in a turn of the route. The SDQ-S is a five-point scale, ranging from "strongly agree (one point)" to "strongly disagree (five points)". Questions 1, 6 and 7, are scored in reverse order. Therefore, the higher score on the SDQ-S indicates higher navigation ability in daily life. The mean score of the SDQ-S in 246 individuals was 56.2 (S.D. = 15.27, range: 19–85). The females demonstrated a significantly lower score of SDQ-S (mean: 53.2; S.D.: 14.4) than males did (mean: 58.6; S.D.: 15.56) (two-sample $t$-test, $p = 0.01$).

Individuals with preferably high and low SDQ-S score ($n = 28$, score $> 60$ and $n = 28$, score $< 39$, respectively) among the applicants were selected in order to obtain a sample with as large a variance on the navigation ability as possible, and then 56 healthy right-handed normal subjects consisting of four groups, 14 male good navigators (mean age and S.D.: 28.6 and 8.8), 14 male poor navigators (26.78 and 6.43), 14 female good navigators (26.7 and 2.98), and 14 female poor navigators (27.85 and 5.32) were selected (no significant difference of age amongst groups). After description of the study, written informed consent was obtained from every subject. The study protocol was approved by the ethics committee of the National Center of Neurology and Psychiatry, Tokyo, Japan and was conducted by the principles of the Declaration of Helsinki. None had a history of neurological or psychiatric disorders or any sign of color blindness, visual field defects or visual-spatial problems. The mean scores (S.D.) of SDQ-S in each group were 34 (7.4) in male poor navigators, 30.6 (6.43) in female poor navigators, 75.33 (7.44) in male good navigators, and 73.5 (8.32) in female good navigators, respectively. The ANOVA, navigation ability (good and poor) by sex, with the score of SDQ-S, revealed only a significant main effects of navigation ability ($F(1, 54) = 52.98$, $p < 0.001$). There is no main effect of sex or interaction effect. The main effect of navigation ability showed that good navigators showed higher scores of SDQ-S than poor navigators did ($p < 0.001$). Five items (questions 1, 2, 4, 6, and 7) of the SDQ-S were considered to be associated with preferred navigation strategy in the daily life; i.e., individuals with higher scores tend to prefer the allocentric orientation strategy, whereas individuals with lower scores tend to have a difficulty in allocentric orientation strategy. We also analyzed the data of five items of of the SDQ-S.

### 2.2. fMRI procedure

Cerebral activation was measured with fMRI using blood oxygen level-dependent contrast. After automatic shimming, a time course series of 140 volumes was obtained using single-shot gradient-refocused echo-planar imaging (TR = 4000 ms, TE = 60 ms, flip angle = 90°, inter-scan interval 4 s, in-plane resolution 3.44 mm × 3.44 mm, FOV = 22 cm, contiguous 4-mm oblique slices to cover the entire brain, slice angle was selected to avoid susceptibility artifact from sphenoid sinus) with a 1.5 T MAGNETOM Vision plus MR scanner (Siemens, Erlangen, Germany) using the standard head coil. The first five volumes of each fMRI scan were discarded because of non-steady magnetization, with the remaining 135 volumes used for the analysis. Before the collection of fMRI data for each subject, we acquired a reference EPI scan and visually inspected it for artifacts (i.e., ghosting) as well as for good signal across the entire volume of acquisition, particularly the medial temporal lobes. Head motion was minimized by placing tight but comfortable foam padding around the subject's head. The fMRI protocol was a block design with nine blocks of virtual maze task, nine blocks of control task and nine blocks resting conditions. Each block lasted 20 s (equivalent to five whole-brain fMRI volume acquisitions).

### 2.3. Navigation tasks

We applied a passive-watching task, watching movies of exploration in mazes, as a navigation task to minimize explicit motor outputs and commands. Nine different simple three-dimensional mazes for task epochs were programmed with a commercially available software program for building design on a PC. The program has a function showing someone walking around a building presented from a first person's view, which is recorded as a movie file. During the task condition, the subjects were asked to watch a 15 s movie of exploration in a maze from the first person point of view, in a three-dimensional, fully textured environment. Fig. 1(left) displays a typical view experienced by subjects within the task condition. Immediately after the movie finished, two maps of the maze from a bird's eye view were presented for 5 s (Fig. 1, right). The one was correct map and another was wrong one. Subjects were asked to judge which map was correct. They used a two-button response box under their right hand to select the answer. To give a correct answer, the subjects have to construct an allocentric 'cognitive map' from egocentric spatial information during watching the movie. The stimuli were presented using Media player running on a PC and backprojected onto a screen, approximately 50-cm from the subject's head, using a 65,536-color liquid crystal display and an overhead projector. The subjects viewed the screen through a mirror attached to the head coil. During the control condition, subjects were asked to watch a movie of walking in a straight passage, which has the same texture as the maze presented during the task epoch. The movement speed was made the same with all task and control epochs. Prior to the fMRI measurement, all subjects were trained on a maze to familiarize with the task.

### 2.4. Data analysis

Data were analyzed with Statistical Parametric Mapping software (SPM2). Scans were realigned and spatially normalized to the standard stereotactic space of Talairach using EPI template. The parameter for affine and quadratic transformation to the EPI template that was already fit for Talairach space was estimated by least-squares means. Data were then smoothed in a spatial domain (full width at half-maxim = 8 mm × 8 mm × 8 mm) to improve the signal to noise ratio. After specifying the appropriate design matrix, delayed box-car function as a reference waveform, the condition, slow hemodynamic fluctuation unrelated to the task, and subject effects were estimated according to

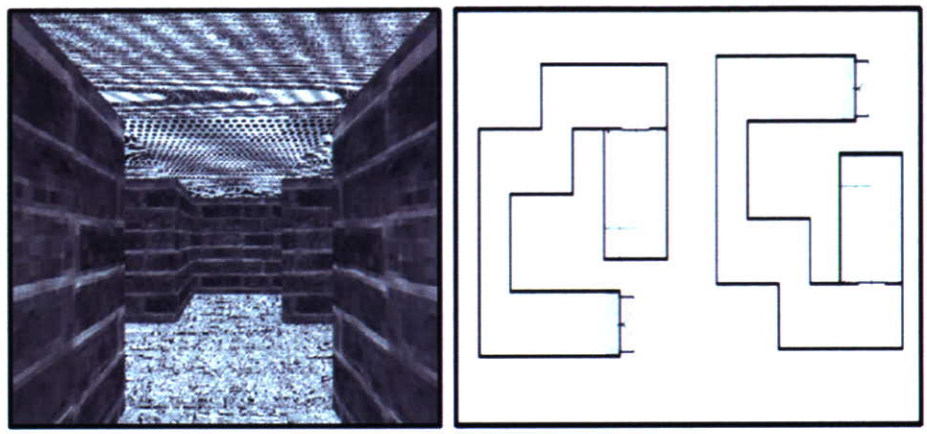

Fig. 1. An example of stimuli for fMRI. Left: typical view from inside the virtual maze. During the task condition, subjects were asked to watch a 15 s movie showing exploration in a maze from a first person point of view, three-dimensional, fully textured environment. Right: immediately after the movie was finished, two maps of the maze were presented for 5 s. During this period, subjects have to choose the correct map.

a general linear model taking temporal smoothness into account. To test hypotheses about regionally specific condition effects, the estimates were compared by means of linear contrasts of each control and task period. The resulting set of voxel values for each contrast constituted a statistical parametric map of the $t$ statistic SPM $\{t\}$. To account for inter-individual variance, all group analyses were computed using a random-effects model (Friston et al., 1999). Group analysis across groups involved a one-sample $t$-test on the images generated by pooling over the session the individual contrasts of task condition versus control condition for each subject. Between groups, regionally specific main effects (navigation ability and sex) and interaction effects were analyzed by analysis of variance design matrix. Furthermore, we performed correlational analyses to find where activation responded to task performance (number of correct answers of the maze task during fMRI measurements, full score was nine points) and scores of five items of the SDQ-S. All the analyses, we used $p < 0.001$, corrected for multiple comparisons with false discovery rate (FDR) $<0.05$ as a statistical threshold. Since a recent human study demonstrated that hippocampus and parahippocampal gyrus differently contributed to spatial navigation (Ekstrom et al., 2003), we additionally performed regression analyses with region of interest analysis (ROI) to clarify whether activation response to task performance and scores of five items of the SDQ-S differ between hippocampus and parahippocampal gyrus. For this hypothesis-driven analysis, we used the Wake Forest University PickAtlas (Maldjian et al., 2003) to make ROIs for hippocampus and parahippocampal gyrus separately and used to marsbar (http://marsbar.sourceforge.net/) to extract values within ROIs. Using the extracted value of each ROI, we performed linear correlational analysis between task performance, scores of five items of the SDQ-S and magnitude of the activation within the ROIs in each region (hippocampus and parahippocampal gyrus), and examined if there were any region by task

Table 1
Brain activity related to maze task in the whole group

| Anatomical region | Broadman area | Talairach coordinate | | | $t$-Value |
|---|---|---|---|---|---|
| | | $X$ | $Y$ | $Z$ | |
| Left | | | | | |
| Parahippocampal gyrus | 30/35/36 | −26 | −30 | −25 | 9.85 |
| Hippocampus | | −20 | −35 | −4 | 5.17 |
| Posterior cingulate gyrus | 30 | −14 | −58 | 7 | 6 |
| Precuneus | 7,19 | −16 | −65 | 51 | 15.68 |
| Cuneus | 17 | −8 | −91 | 3 | 9.36 |
| Superior parietal lobule | 7 | −14 | −61 | 53 | 13 |
| Inferior parietal lobule | 40 | −36 | −39 | 41 | 9.3 |
| Fusiform gyrus | 19/37 | −44 | −63 | −22 | 10.15 |
| Middle occipital gyrus | 18/19 | −44 | −81 | 10 | 13.38 |
| Superior colliculus | | −3 | −35 | −3 | 5.98 |
| Right | | | | | |
| Parahippocampal gyrus | 30/35/36 | 34 | −38 | −27 | 10 |
| Hippocampus | | 21 | −37 | −5 | 5.22 |
| Posterior cingulate gyrus | 29/30/31 | 20 | −57 | 19 | 8.32 |
| Precuneus | 7,19 | 16 | −65 | 53 | 16.85 |
| Cuneus | 17 | 16 | −97 | 3 | 14.55 |
| Superior parietal lobule | 7 | 30 | −56 | 53 | 11.1 |
| Inferior parietal lobule | 40 | 36 | −45 | 41 | 8.34 |
| Fusiform gyrus | 19/37 | 32 | −59 | −17 | 11.3 |
| Middle occipital gyrus | 18/19 | 50 | −68 | −5 | 12.28 |
| Lingual gyrus | 17/18 | 12 | −80 | −8 | 12.98 |
| Superior colliculus | | 3 | −22 | −4 | 5.96 |
| Middle frontal gyrus | 9 | 51 | 16 | 26 | 11.86 |